Journal of Power Sources 268 (2014) 50–55

Contents lists available at ScienceDirect

Journal of Power Sources

journal homepage: www.elsevier.com/locate/jpowsour

Corrosion protection of aluminum bipolar plates with polyaniline coating containing carbon nanotubes in acidic medium inside the polymer electrolyte membrane fuel cell

M.A. Deyab*

Egyptian Petroleum Research Institute (EPRI), Nasr City, Cairo, Egypt

HIGHLIGHTS

- We examine the effect of addition of CNTs on the corrosion resistance of polyaniline in PEM fuel cell.
- The addition of CNTs to polyaniline coating enhanced conductivity of polyaniline.
- The addition of CNTs increases the inhibition efficiency of polyaniline coating.
- Inhibition efficiency is close to 98% when CNTs concentration is 0.8%.
- The techniques include electrical conductivity, polarization, EIS and SEM.

GRAPHICAL ABSTRACT

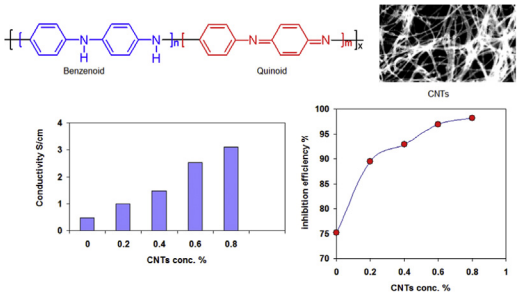

ARTICLE INFO

Article history:
Received 4 February 2014
Received in revised form
22 April 2014
Accepted 4 June 2014
Available online 12 June 2014

Keywords:
Carbon nanotubes
Conductive polymer
Aluminum
Corrosion
Coating

ABSTRACT

The effect of addition of carbon nanotubes (CNTs) on the corrosion resistance of conductive polymer coating (polyaniline) that coated aluminum bipolar plates in acidic environment inside the PEM fuel cell (0.1 M H_2SO_4) was investigated using electrical conductivity, polarization and electrochemical impedance spectroscopy (EIS) measurements. Scanning electron microscopy (SEM) was used to characterize the coating morphology. The results show that the addition of CNTs to polyaniline coating enhanced the electrical conductivity and the corrosion resistance of polyaniline polymer. The inhibition efficiency of polyaniline polymer increased with increasing CNTs concentration. The best inhibition was generally obtained at 0.8% CNTs concentration in the acidic medium. This was further confirmed by decreasing the oxygen and water permeability and increasing coating adhesion in the presence of CNTs. EIS measurements indicated that the incorporation of CNTs in coating increased both the charge transfer and pore resistances while reducing the double layer capacitance.

1. Introduction

Polymer electrolyte membrane (PEM) fuel cells are a type of fuel cell being developed for transport applications as well as for stationary fuel cell applications and portable fuel cell applications [1]. PEM fuel cell transforms the chemical energy liberated during the electrochemical reaction of hydrogen and oxygen to electrical energy, as opposed to the direct combustion of hydrogen and oxygen gases to produce thermal energy [2]. A stream of hydrogen is delivered to the anode side of the membrane electrode assembly (MEA). At the anode side it is catalytically split into protons and electrons. This oxidation half-cell reaction is represented by [3]:

* Tel.: +20 1006137150; fax: +20 2 22747433.
E-mail address: hamadadeiab@yahoo.com.

http://dx.doi.org/10.1016/j.jpowsour.2014.06.021
0378-7753/

$$H_2 \rightarrow 2H^+ + 2e \text{ (at the anode)} \quad (1)$$

The newly formed protons permeate through the polymer electrolyte membrane to the cathode side. The electrons travel along an external load circuit to the cathode side of the MEA, thus creating the current output of the fuel cell. Meanwhile, a stream of oxygen is delivered to the cathode side of the MEA. At the cathode side oxygen molecules react with the protons permeating through the polymer electrolyte membrane and the electrons arriving through the external circuit to form water molecules. This reduction (half-cell reaction) is represented by:

$$1/2O_2 + 2H^+ + 2e \rightarrow H_2O \text{ (at the cathode)} \quad (2)$$

The polymer membrane must conduct hydrogen ions (protons) but not electrons as this would in effect "short circuit" the fuel cell. The membrane must also not allow either gas to pass to the other side of the cell. Finally, the membrane must be resistant to the reducing environment at the cathode as well as the harsh oxidative environment at the anode [4].

The bipolar plates perform as the current conductors between cells, provide conduits for reactant gases flow, and constitute the backbone of a power stack [5]. They are commonly made of graphite composite for high corrosion resistance and good surface contact resistance; however their manufacturability, permeability, and durability for shock and vibration are unfavorable in comparison to metals [5].

Increasing attention is being paid to the use of metallic materials such as Fe, Al, Cu, Ni, Ti-based alloys in bipolar plates for PEM fuel cells [6–9]. Aluminum and its alloys have excellent physical and chemical properties and presently find extensive industrial as well as domestic applications and in spite of this, there is a few of work reported on using Aluminum bipolar plates [10].

Metals should demonstrate higher mechanical strength, higher values of electrical conductivity, better durability to shocks and vibration, no permeability, and much superior manufacturability and cost effectiveness when compared to graphite composite. However, the main disadvantage of metals is the lack of ability to resist corrosion in the harsh acidic and humid environment inside the PEM fuel cell [11]. The corrosion of bipolar plates causes the membrane poisoning and lowers the ionic conductivity of the membrane and this lead to lower the PEM fuel cell performance [12].

Several coating materials and processes have been proposed to improve the corrosion resistance of metals in the PEM environment [13–15]. One such material is a conducting polymer coating [16,17].

Conductive polymers are organic polymers that conduct electricity. Such compounds may have metallic conductivity or can be semiconductors. Conducting polymers can combine the electronic characteristics of metals with the engineering properties of polymers. Polypyrrole, polythiophene and polyaniline are common examples of conducting polymers [18].

A carbon nanotubes (CNTs) is a tube-shaped material, made of carbon, having a diameter measuring on the nanometer scale [19]. Carbon nanotubes have attracted the fancy of many scientists worldwide. The small dimensions, strength and the remarkable physical properties of these structures make them a very unique material with a whole range of promising applications. One method to improve the corrosion resistance and conductivity provided by conductive polymers coatings is the addition of carbon nanotube [20].

The aim of this work is to study the effect of addition of CNTs on the corrosion resistance of conductive polymer coating (polyaniline) that coated aluminum bipolar plates in acidic environment inside the PEM fuel cell (0.1 M H_2SO_4).

2. Experimental

2.1. Materials

Corrosion tests were performed on aluminum sheets of the following percentage composition: Al (99.89%), Si (0.03%), Cu (0.02%), Mg (0.03%) and Zn (0.01%). Prior to each experiment, the aluminum electrode with dimension 12 × 17 × 0.5 mm were first briefly ground with different grades of emery paper (120, 400, 800, 1000 and 1200) and washed thoroughly with distilled water and degreased with acetone.

Polyaniline polymer was obtained from Sigma–Aldrich Co. Xylene was received from Sciencelab.com, Inc. and used without further purification.

Carbon nanotubes CNTs that were prepared by Egyptian Petroleum Research Institute (EPRI) (diameter: 20–30 nm, length: 1–10 μm, layers: 5–20).

The aggressive solutions, 0.1 M H_2SO_4 were prepared by dilution of AR grade 98% H_2SO_4 with distilled water.

2.2. Preparation of polyaniline polymer coating

Painting of polyaniline polymer coating on aluminum was accomplished by dissolving polyaniline polymer in xylene, 1:1 ratio. The dissolved polyaniline polymer was applied on the cleaned aluminum samples by a small brush and dried overnight. The dried samples were heated at 110 °C for 5 min to remove any air bubbles that may have trapped in the coating. The coating thickness measured was 10–12 μm.

Different concentrations (0.2, 0.4, 0.6 and 0.8% by weight) of CNTs powder (average particle size = 20–30 nm) were mixed with 5% of chloroform and then they added to polyaniline polymer coating. The particles were dispersed by using a high speed mechanical stirrer. The electrical conductivity of polyaniline polymer coating in the absence and presence of CNTs was measured by using four point probe method.

The morphology of CNTs and polyaniline coating in the absence and presences of 0.8% CNTs were performed recorded using JEOL-JEM 1200 EX II scan electron microscope (SEM).

2.3. Electrochemical measurements

Electrochemical experiments were carried out in a conventional three-electrode cell with a platinum counter electrode and a saturated calomel electrode (SCE) coupled to a fine Luggin capillary as the reference electrode. To minimize the ohmic contribution, the Luggin capillary was kept close to aluminum (working electrode). Electrochemical measurements were performed using Gill AC Serial no. 947 (ACM instruments).

Potentiodynamic polarization measurements were carried out at potential range of ±200 mV with respect to the corrosion potential (E_{corr}) at a sweep rate of 0.125 mV s^{-1}. The linear Tafel segments of the anodic and cathodic curves were extrapolated to corrosion potential to obtain the corrosion current densities (j_{corr}).

EIS measurements were carried out using AC signals of amplitude 5 mV peak to peak at the open-circuit potential in the frequency range 100 kHz to 10 mHz.

2.4. Coating adhesion and permeability measurements

For Adhesion test, coated carbon steel panels were submitted to the pull-off test using the Elcometer tester model 107 (CORRPRO CO. INC.).

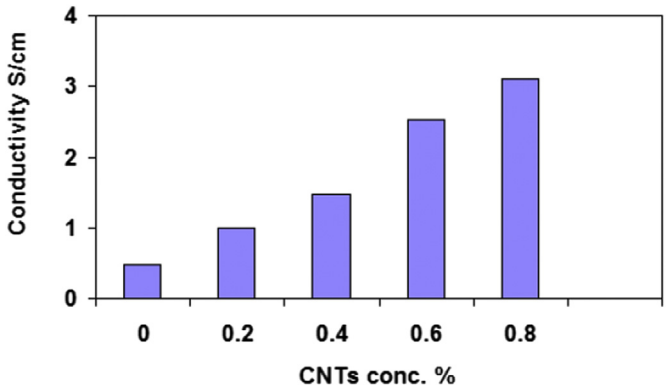

Fig. 1. The electrical conductivity of polyaniline coating versus of CNTs concentration.

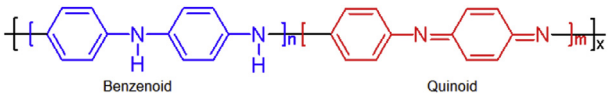

Fig. 2. Main polyaniline structures n + m = 1, x = degree of polymerization.

Oxygen and water permeability of prepared coating were determined at 298 K using Oxygen Permeation Analyzers (model 8501, Illinois Instruments, Inc.) and BYK-Gardner Permeability Cup (BYK Additives & Instruments), respectively.

3. Results and discussion

3.1. Electrical conductivity

Fig. 1 provides the specific electrical conductivity of polyaniline coating as function of CNTs content. The data reveal that the addition of CNTs to polyaniline coating enhanced conductivity of polyaniline coating. Furthermore, the conductivity increases with increasing CNTs content.

Polyaniline consist two kinds of rings (Fig. 2), quinoid ring with hybridized orbitals, which is resonance stabilized and it enables charge transport between chains, while benzenoid rings are non-conductive in nature. The enhancement in the conductivity of polyaniline coating in the presences of CNTs is due to the charge transfer effect from the quinoid rings of the polyaniline to the CNTs. Furthermore, the CNTs may serve as "conducting bridges", connecting the polyaniline conducting domains [21].

SEM images of CNTs and polyaniline coating in the absence and presences of 0.8% CNTs are shown in Fig. 3a, b and c respectively. Rough surface and increased diameter of the composite (Fig. 3c) indicated the coating of polyaniline polymer (Fig. 3b) over the CNTs (Fig. 3a). SEM image (Fig. 3c) shows also the homogeneous coating of polyaniline polymer onto the CNTs, indicating that CNTs were well dispersed in polymer matrix. Fig. 3c shows new interwoven fibrous structure which acts as conductive pathway and lead to high conductivity than that of pure polyaniline polymer (Fig. 3b).

3.2. Corrosion testing after coating with polyaniline polymer

3.2.1. Polarization measurements

In order to determine the corrosion resistance performance of polyaniline polymer coating in the absence and presence of CNTs, potentiodynamic polarization tests were conducted on uncoated (Blank) and coated aluminum bipolar plates in 0.1 M H_2SO_4 in the absence and presence of different concentrations of CNTs (0.2–0.8%) at 298 K (Fig. 4). It can be noticed From Fig. 4 that the polyaniline polymer coating causes a remarkable shift in the corrosion potential (E_{corr}) to more positive value and shift both anodic and cathodic Tafel curves to lower current densities. The values of the corrosion current density (j_{corr}) for aluminum corrosion reaction were determined by extrapolation of the cathodic and anodic Tafel lines to the corrosion potential E_{corr}. The electrochemical parameters such as corrosion potential E_{corr}, and corrosion current density j_{corr} obtained by extrapolating the Tafel line are given in Table 1.

The inhibition efficiency (η_j) has been calculated with Eq. (3) and the values obtained are presented in Table 1:

$$\eta_j\% = \frac{j_{corr(uncoated)} - j_{corr(coated)}}{j_{corr(uncoated)}} \times 100 \quad (3)$$

where $j_{corr\ (uncoated)}$ and $j_{corr\ (coated)}$ represent the current density values of the uncoated and coated aluminum, respectively.

Table 1 shows that the polyaniline polymer coating caused a remarkable potential shift −0.398 V versus SCE in the corrosion potential (E_{corr}), relative to the value of the uncoated aluminum (−0.608 V). The positive shift in E_{corr} confirms the best protection of the aluminum when its surface is covered by the polyaniline polymer coating [22].

It reveals from Table 1 that the corrosion current density j_{corr} was suppressed in coated aluminum compared to uncoated aluminum. On other hand, the suppression in j_{corr} values increase in the presence of CNTs.

The inhibition efficiency of polyaniline polymer coating in the absence of CNTs is initially 75.2% and increased drastically to 89.5% in the presence of 0.2% CNTs. However, with further increasing CNTs concentration, the inhibition efficiency increases. The maximum inhibition efficiency (98.2%) is at 0.8% CNTs.

This behavior can be explained on the basis that polyaniline polymer coating is widely used to preventing oxygen and corrosive solution form reaching the surface of metal. In the same time polyaniline polymer coating isolate the aluminum surface form the corrosive medium.

The main disadvantage of coating film is the permeability of coating for oxygen or corrosive solution [23]. The permeability of coating for corrosive solution or oxygen depends primarily on the molecular structure and chemical nature of the binder, especially

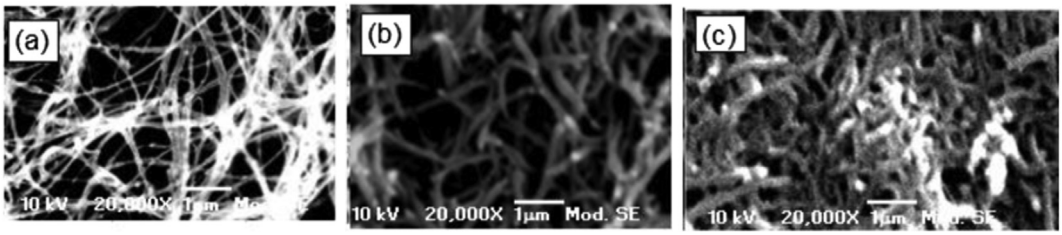

Fig. 3. SEM images of CNTs (a), polyaniline polymer (b) and polyaniline polymer in the presences of 0.8% CNTs (c).

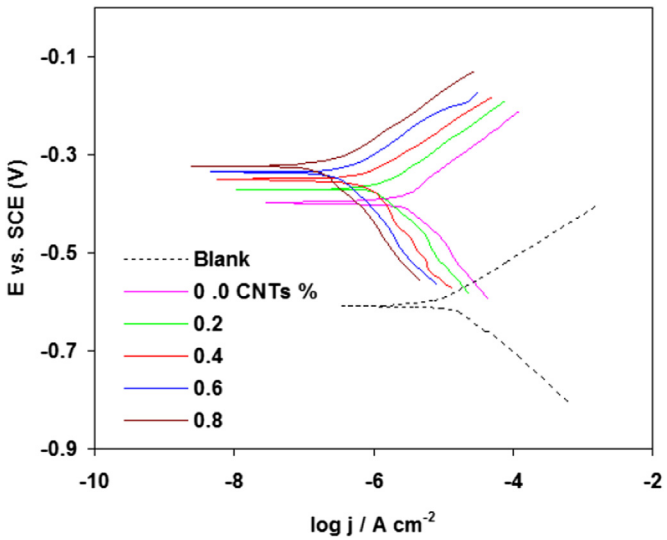

Fig. 4. Potentiodynamic polarization curves for uncoated (Blank) and coated aluminum bipolar plates in 0.1 M H_2SO_4 in the absence and presence of different concentrations of CNTs at 298 K.

the degree of cross-linking [24]. For good corrosion protection, an organic coating should have the smallest permeability possible. The data clearly show that in the absence of CNTs the coating film does not completely prevent oxygen and corrosive solution form reaching the metal surface. On the other hand, addition of CNTs leads to decrease the permeability of coating for oxygen and corrosive solution and this in turn leads to greater corrosion inhibition [25]. This explanation can be supported by determining the permeability of polyaniline polymer coating for oxygen and water (Table 2). From Table 2, it can be observe that the incorporation of CNTs into polyaniline polymer coating leads to the decrease in oxygen and water permeability. Furthermore, the values of oxygen and water permeability decreased with increasing CNTs concentration.

Besides the permeability factor, coatings have been modified with CNTs to achieve desirable properties such as increased adhesion and cohesion [26,27]. The coating adhesion between the coating and aluminum surface after immersion of coated aluminum in 0.1 M H_2SO_4 in the absence and presence of different concentrations of CNTs at 298 K is shown in Table 3. It can be seen that the value of coating adhesion between the coating and aluminum surface increased with increasing CNTs concentration, confirming the suggestion that incorporation of CNTs into polyaniline polymer coating provide better adhesion and this in turn leads to greater corrosion resistance.

3.2.2. EIS measurements

EIS is probably the most important electrochemical technique used for the investigation of coatings for metals corrosion protection in industrial applications [28]. The Nyquist impedance plot of

Table 1
Electrochemical parameters and the corresponding inhibition efficiency for uncoated (Blank) and coated aluminum bipolar plates in 0.1 M H_2SO_4 in the absence and presence of different concentrations of CNTs at 298 K.

CNTs (%)	E_{corr} (V vs. SCE)	j_{corr} (μA cm^{-2})	η_i %
Blank	−0.608	10.22	–
0.0	−0.398	2.53	75.2
0.2	−0.371	1.07	89.5
0.4	−0.349	0.72	92.9
0.6	−0.335	0.31	96.9
0.8	−0.324	0.18	98.2

Table 2
Oxygen and water permeability of coating in the absence and presence of CNTs at 298 K.

CNTs (%)	O_2 permeability cc m^{-2} day	H_2O permeability g m^{-2} day
0.0	8.22	1.07
0.2	5.94	0.58
0.4	2.51	0.24
0.6	1.08	0.19
0.8	0.58	0.12

Table 3
The coating adhesion between the coating and aluminum in the absence and presence of CNTs at 298 K.

CNTs (%)	Coating adhesion (Kg cm^{-2})
0.0	13
0.2	18
0.4	20
0.6	24
0.8	30

uncoated aluminum after 7 days immersion in 0.1 M H_2SO_4 at 298 K is shown in Fig. 5. The impedance spectra exhibits one single depressed semicircle, this indicates that the charge transfer takes place at electrode/solution interface [29].This impedance plot was modeled by the equivalent circuit depicted in Fig. 6. The equivalent circuit consists of the electrolyte resistance (R_s), charge-transfer resistance (R_{ct}) and double layer capacitance (C_{dl}). The double layer capacitance is in parallel with the charge transfer resistance.

The Nyquist impedance plots of polyaniline polymer coated aluminum in the absence and presence of CNTs at 298 K are shown in Fig. 7. This impedance plot is modeled by using the equivalent circuit depicted in Fig. 8, which consists of the electrolyte resistance (R_s), pore resistance (R_p), coating capacitance (C_c), charge-transfer resistance (R_{ct}) and double layer capacitance (C_{dl}). The capacitance of the intact coating is represented by C_c. Its value is much smaller than a typical double layer capacitance. R_{po} (pore resistance) is the resistance of ion conducting paths across the coating [30]. These paths may not be physical pores filled with electrolyte. On the metal side of the pore, we assume that an area of the coating has delaminated and a pocket filled with an electrolyte solution has formed [31]. This electrolyte solution can be very different than the

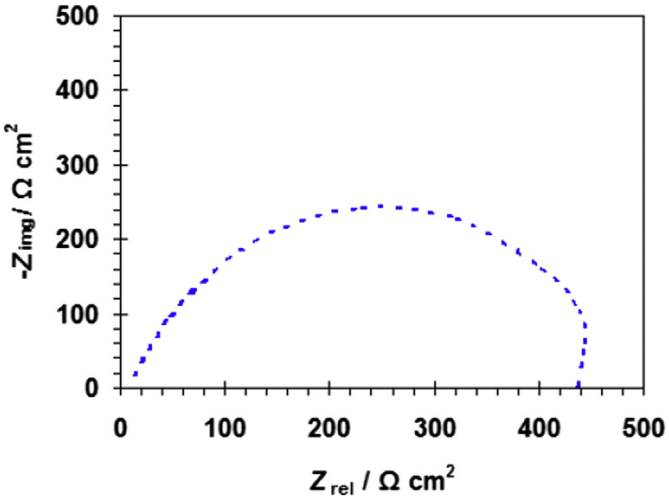

Fig. 5. The Nyquist impedance plot of uncoated aluminum after 7 days immersion in 0.1 M H_2SO_4 at 298 K.

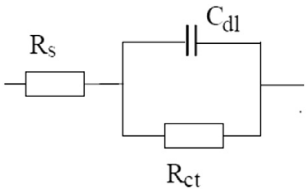

Fig. 6. Equivalent electrical circuit for uncoated aluminum.

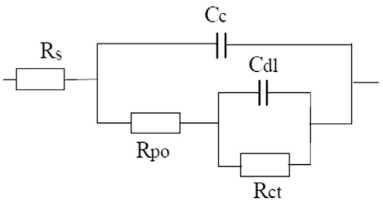

Fig. 8. Equivalent electrical circuit for coated aluminum.

bulk solution outside of the coating. The interface between this pocket of solution and the bare metal is modeled as a double layer capacitance in parallel with a kinetically controlled charge transfer reaction [31].

The impedance plot of polyaniline polymer coating coated aluminum can be fitted with two semicircles, a smaller one at high frequency range followed by a larger one at lower frequencies. The first semicircle is attributed to the polyaniline polymer coating itself and the second one to processes occurring underneath the coating [32].

Table 4 shows the impedance parameters recorded for uncoated (Blank) and coated aluminum bipolar plates in 0.1 M H_2SO_4 in the absence and presence of different concentrations of CNTs (0.2–0.8%) at 298 K. The data shows that The R_{ct} value of coated aluminum is higher than that of the uncoated aluminum. The higher value of R_{ct} is attributed to the effective barrier behavior of the polyaniline polymer coating. Furthermore, the value of R_{ct} increases with increasing CNTs concentration. This confirms that the impedance of coated aluminum by polyaniline polymer increases with CNTs concentration. The lower values of C_{dl} for the coated aluminum provide further support the protection of aluminum by polyaniline polymer coating. The decrease in C_{dl} with an increase in CNTs concentration is attributed to the higher protective layer of polyaniline polymer coating on the aluminum surface [33].

It is clear form Table 4 that the Incorporation of CNTs into polyaniline polymer coating increased R_{po} values. Moreover, the value of R_{po} increases with increasing CNTs concentration. The increase in R_{po} values in the presence of CNTs, likely due to the decrease in coating porosity [34]. In addition, the porosity of coating decreases with increasing CNTs concentration.

That EIS data suggest that the two thinkable mechanisms share in the enhanced corrosion protection of polyaniline polymer coating in the presence of CNTs. First, CNTs reduce the porosity of the coating matrix and inhibit the ions and water penetration into the coating and subsequent electrochemical reactions at the coating/metal interface, leading to improved barrier performance of polyaniline polymer coating. Second, CNTs improve the adherence of polyaniline polymer coating to the metal surface [34].

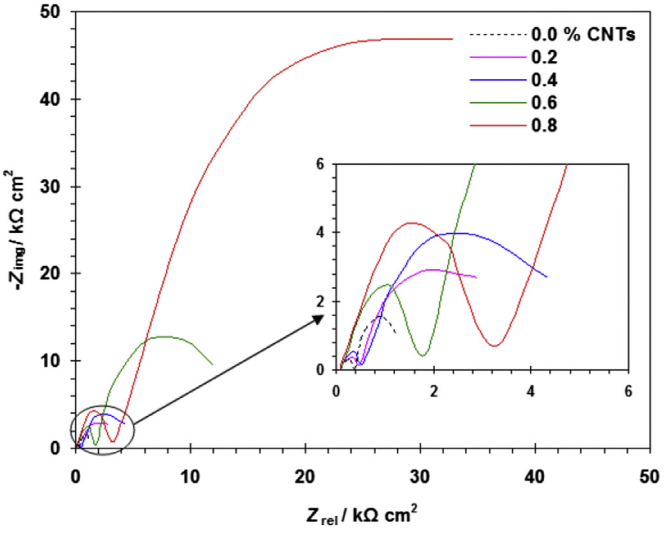

Fig. 7. The Nyquist impedance plots for coated aluminum with polyaniline polymer in the absence and presence of CNTs at 298 K.

Table 4
Impedance parameters and the corresponding inhibition efficiency for uncoated (Blank) and coated aluminum bipolar plates in 0.1 M H_2SO_4 in the absence and presence of different concentrations of CNTs at 298 K.

CNT %	R_{CT} (kΩ cm^2)	R_{po} (kΩ cm^2)	C_{dl} (F cm^{-2})	η_R %
Blank	0.43	–	3.70×10^{-5}	–
0.0	1.95	0.39	4.08×10^{-6}	77.94
0.2	4.35	0.50	1.83×10^{-6}	90.11
0.4	7.28	0.68	1.09×10^{-6}	94.09
0.6	17.55	1.82	4.53×10^{-7}	97.54
0.8	72.83	3.25	1.09×10^{-7}	99.40

From the R_{ct} values, the inhibition efficiency (η_R%) values were determined from the equation:

$$\eta_R\% = \frac{R_{(coated)} - R_{(uncoated)}}{R_{(coated)}} \times 100 \quad (4)$$

where $R_{ct(coated)}$ and $R_{ct(uncoated)}$ are the charge transfer resistance of coated and uncoated aluminum. The calculated values of η_R% also are given in Table 4. The inhibition efficiency η_R% was found to increase with increase in CNTs concentration and the maximum inhibition efficiency (η_R% = 99.40%) was obtained at 0.8% CNT. The inhibition efficiency values obtained for the Polarization and EIS measurements are in good agreement.

4. Summary

1. Conductive polymer coating (polyaniline) has great potential to prevent aluminum bipolar plates from corrosion attack in acidic environment.
2. The addition of CNTs to polyaniline coating enhanced conductivity of polyaniline coating.
3. SEM images show a uniform distribution of CNTs in polyaniline, indicating that the CNTs are well dispersed in the composites.
4. The corrosion rate was suppressed in coated aluminum compared to uncoated aluminum. On other hand, the suppression in the corrosion rate increase in the presence of CNTs.
5. The addition of CNTs increases the inhibition efficiency of polyaniline coating. The maximum inhibition efficiency (98.2%) is at 0.8% CNTs.
6. The addition of CNTs increases the adhesion strength of coating, and decreases the oxygen and water permeability.
7. The EIS measurements indicated that the incorporation of CNTs increased the charge transfer and pore resistances while reducing the double layer capacitance.
8. The results obtained from polarization and impedance studies are in a good agreement

References

[1] J.S. Lee, N.D. Quan, J.M. Hwang, S.D. Lee, H. Kim, H. Lee, H.S. Kim, J. Ind. Eng. Chem. 12 (2006) 175–183.
[2] G. Hoogers, Fuel Cell Technology Handbook, CRC Press, Boca Raton, FL, 2003.
[3] X.Z. Yuan, C. Song, H. Wang, J. Zhang, Electrochemical Impedance Spectroscopy in PEM Fuel Cells – Fundamentals and Applications, Springer, London, 2010.
[4] R. Esposito, A. Conti, Polymer Electrolyte Membrane Fuel Cells and Electrocatalysts, Nova Science Publishers, 2009.
[5] H. Tawfik, Y. Hunga, D. Mahajan, J. Power Sources 163 (2007) 755–767.
[6] S.-H. Wang, J. Peng, W.-B. Lui, J.-S. Zhang, J. Power Sources 162 (2006) 486–491.
[7] S.-H. Wang, J. Peng, W.-B. Lui, J. Power Sources 160 (2006) 485–489.
[8] J.R. Mawdsley, J.D. Carter, X. Wang, S. Niyogi, C.Q. Fan, R. Koc, G. Osterhout, J. Power Sources 231 (2013) 106–112.
[9] R.A. Antunes, M. Cristina, L. Oliveira, G. Ett, V. Ett, Int. J. Hydrogen Energy 35 (2010) 3632–3647.
[10] S. Joseph, J.C. McClure, P.J. Sebastian, J. Moreira, E. Valenzuela, J. Power Sources 177 (2008) 161–166.
[11] Y. Hung, H. Tawfik, D. Mahajan, Smart Grid Renew. Energy 4 (2013) 43–47.
[12] T. Cheng, in: D.P. Wilkinson, J. Zhang, R. Hui, J. Fergus, X. Li (Eds.), Proton Exchange Membrane Fuel Cells: Materials Properties and Performance, Taylor & Francis Group, Boca Raton, Fla, USA, 2010, pp. 307–326.
[13] Y. Wang, D.O. Northwood, J. Power Sources 175 (2008) 40–48.
[14] M.A.L. García, M.A. Smit, J. Power Sources 158 (2006) 397–402.
[15] L. Wang, D.O. Northwood, X. Nie, J. Housden, E. Spain, A. Leyland, A. Matthews, J. Power Sources 195 (2010) 3814–3821.
[16] André Wolz, Susanne Zils, Marc Michel, Christina Roth, J. Power Sources 195 (2010) 8162–8167.
[17] C.-H. Lee, Y.-B. Lee, K.-M. Kim, M.-G. Jeong, D.-S. Lim, Renew. Energy 54 (2013) 46–50.
[18] T.K. Das, S. Prusty, Polym.-Plast. Technol. Eng. 51 (2012) 1487–1500.
[19] R. Angelucci, R. Rizzoli, V. Vinciguerra, M. Fortuna Bevilacqua, S. Guerri, F. Corticelli, M. Passini, Phys. E Low-dimensional Syst. Nanostructures 7 (2007) 11–15.
[20] Y.-B. Lee, C.-H. Lee, D.-S. Lim, Int. J. Hydrogen Energy 34 (2009) 9781–9787.
[21] B. Kondawar, S.W. Anwane, D.V. Nandanwar, S.R. Dhakate, Adv. Mat. Lett. 4 (2013) 35–38.
[22] C.K. Tan, D.J. Blackwood, Corros. Sci. 45 (2003) 545–557.
[23] J.-M. Yeh, S.-J. Liou, C.-G. Lin, Y.-P. Chang, Y.-H. Yu, C.-F. Cheng, J. Appl. Polym. Sci. 92 (2004) 1970–1976.
[24] G.P.A. Turner, Introduction to Paint Chemistry and Principles of Paint Technology, Chapman & Hall, New York, USA, 1988.
[25] M.A. Deyab, S.T. Keera, Mater. Chem. Phys. 146 (2014) 406–411.
[26] S. Ganguli, H. Aglan, P. Dennig, J. Reinf, Plast. Compos. 25 (2006) 175–188.
[27] H.R. Jeon, J.H. Park, M.Y. Shon, J. Ind. Eng. Chem. 19 (2013) 849–853.
[28] E. Cano, D. Lafuente, D.M. Bastidas, J. Solid State Electrochem. 14 (2010) 381–391.
[29] M.A. Deyab, Int. J. Hydrogen Energy 38 (2013) 13511–13519.
[30] A.G. Bailey, J. Electrostat. 45 (1998) 85–120.
[31] M. Kendig, J. Scully, Corrosion 46 (1990) 22–29.
[32] P. Pawar, A.B. Gaikawad, P.P. Patil, Sci. Tech. Adv. Mater. 7 (2006) 732–744.
[33] E. Barsonkov, J.R. Macdonald, Impedance Spectroscopy: Theory, Experiment and Applications, second ed., Wiley-Interscience, 2005.
[34] X. Shi, T.A. Nguyen, Z. Suo, Y. Liu, R. Avci, Surf. Coat. Technol. 204 (2009) 237–245.